

^{59}Co NMR studies of metallic NaCo_2O_4

R. Ray, A. Ghoshray, and K. Ghoshray

Solid State and Molecular Physics Division, Saha Institute of Nuclear Physics, 1/AF Bidhannagar, Calcutta 700 064, India

S. Nakamura

Department of Physics, Teikyo University, 1-1 Toyosatodai, Utsunomiya 320-8551, Japan

(Received 3 September 1998; revised manuscript received 4 December 1998)

^{59}Co NMR studies have been performed in metallic NaCo_2O_4 in the temperature range 350–100 K. The powder patterns predominantly correspond to typical second-order quadrupolar splitted central transition of two inequivalent cobalt sites. Features of magnetic interaction are also present. The analysis of the NMR line shape shows that the electric field gradient (EFG) experienced by one of the two sites (site 1) is independent of temperature, whereas around 47% increment in EFG has been observed for site 2 as the temperature is lowered from 350 to 100 K. ^{59}Co NMR shift for each site is almost isotropic in character which varies linearly with susceptibility and basically consists of two parts. Both the sites suffer a large temperature independent shift due to the contribution from orbital paramagnetism (χ_{ov}) which is analogous in metals to the Van Vleck paramagnetic susceptibility. The temperature-dependent Knight shift for site 1 reveals a negative hyperfine coupling constant (A_{hf}^d) arising from inner s core polarization by the d electrons which are itinerant in character. A positive A_{hf}^d observed for site 2 cannot be interpreted directly in a metallic system such as NaCo_2O_4 . A comparison of the magnitude of A_{hf}^d with those of other cobalt oxides suggests that the nucleus which is being probed by NMR, belongs to a diamagnetic cobalt state. Thus the present NMR results together with the susceptibility indicate the presence of Co^{3+} ion with $S = 0$ and the magnetic Co^{4+} ion.

[S0163-1829(99)01314-4]

I. INTRODUCTION

The $3d$ transition metal oxides have attracted renewed attention since the discovery of high-temperature superconducting (HTSC) oxides. As a result of it new materials and new phenomena are being discovered.¹ Much before the discovery of copper based HTSC's, superconductivity has been found in the transition metal oxide having spinel structure such as LiTi_2O_4 with $T_c = 13.7$ K.² Of the known spinels with trivalent titanium, MgTi_2O_4 is one of the most studied compounds although its electrical properties are still unclear.³ Among the several hundred known oxide spinel compounds, few are known to exhibit a metallic electronic ground state at low temperature. LiV_2O_4 is one of them.² Interestingly, it is found⁴ to exhibit heavy fermion behavior characteristic of those of the heaviest mass f -electron systems.⁵ In addition to the spinel oxides, superconductivity has also been found in the layered perovskites such as Sr_2RuO_4 .⁶ This discovery demonstrates that the presence of copper is not a prerequisite for the existence of superconductivity in a layered perovskite. The basic understanding of the conduction mechanism of the conducting transition metal oxides may be helpful to elucidate the concept of superconductivity in HTSC's, which is even now not clear.

As a reference of HTSC's, the alkali cobalt oxides NaCo_2O_4 and KCo_2O_4 are being investigated extensively as they exhibit metallic conduction.^{7,8} They belong to a bronze-type compound expressed as A_xBO_2 ($0.5 \leq x \leq 1$)⁹ and have layered structure where Na (or K) (50% occupied) and CoO_2 are alternately stacked along the c axis. Each Co ion is surrounded by slightly distorted oxygen octahedra. Though the

oxidation state of the cobalt ion is not known unambiguously it is generally assumed that they contain equal amount of Co^{3+} and Co^{4+} ions. In the octahedral ligands $3d$ spins of Co^{3+} and Co^{4+} ions are presumably in the low spin state with $S = 0$ and $S = 1/2$, respectively. Susceptibility measurements show that both of them exhibit Curie Weiss behavior.^{7,8} Assuming that only Co^{4+} spins contribute to the Curie constant in case of KCo_2O_4 , the effective magnetic moment was calculated to be about $0.8\mu_B$.⁸ This value is smaller than $1.73\mu_B$ which is the spin only value of a free atom with $S = 1/2$. However, such calculation was not attempted in case of NaCo_2O_4 .

Recent measurement¹⁰ of thermoelectric power and resistivity of single crystal NaCo_2O_4 has unfolded its technological importance. Interestingly it exhibits one order of magnitude larger thermoelectric power ($100 \mu\text{V/K}$ at 300 K) than typical metals and HTSC's, while it has a low resistivity (ρ_a) ($200 \mu\Omega \text{ cm}$ at 300 K) as HTSC's. The large thermoelectric power accompanied by low ρ_a suggests that NaCo_2O_4 is applicable to thermoelectric devices which convert heat into electric energy through the thermoelectric power of solids. It should also be noted that the results show a strong anisotropy between in-plane (ρ_a) and out of plane (ρ_c) resistivity both in magnitude and in the nature of temperature variation. ρ_c shows a crossover from semiconducting to metallic phase around 200 K with the decrease in temperature, whereas ρ_a shows metallic conduction through all temperatures.

In order to understand the conduction mechanism of this technologically important two-dimensional oxide an extensive investigation of the electronic structure of the octahe-

drally coordinated Co ions is needed. NMR being a microscopic tool will be helpful to investigate the electronic states locally. In this paper, the results of systematic ^{59}Co NMR studies have been reported. The present investigation is concerned primarily with the studies of the paramagnetic properties of metallic NaCo_2O_4 . New susceptibility (χ) data have also been presented. The contributions to the susceptibility from Van Vleck term and d -band spin paramagnetism are obtained from susceptibility data and are compared by studying the ^{59}Co NMR frequency shift as a function of susceptibility. Lastly, the nature of the oxidation state of the cobalt ion in this system would be discussed.

II. EXPERIMENTAL RESULTS

Fresh polycrystalline specimens of NaCo_2O_4 were prepared in two lots and characterized as mentioned in the work of Tanaka *et al.*⁷ Susceptibility data were taken in a superconducting quantum interference device (SQUID) magnetometer at 100 Oersted. For NMR measurements powdered sample were kept in a sealed glass tube filled with pure argon. Both ^{59}Co and ^{23}Na NMR signals were observed, however, we shall discuss here only ^{59}Co NMR results. Since, the oxidation state of the cobalt ion is not known unambiguously, we at present will not assign the ^{59}Co NMR spectra to any particular type of cobalt ion. Assignment will be made as a consequence of the behavior of the observed NMR parameters (Sec. IVB).

^{59}Co NMR spectra are obtained in the field-sweep mode using Varian Associates WL210 nuclear induction spectrometer combined with a Varian V7400 electromagnet. First derivatives of the absorption lines have been recorded at a fixed resonating frequency (ν_R) which lies in the range 14–18 MHz. Investigations are made in the temperature range 350–100 K. Temperature variation is achieved by controlling the temperature of the precooled stream of nitrogen gas, using a Varian V4540 temperature controller. Experiments at different frequencies have been performed to confirm the absence of any trace amount of Co_3O_4 which may be present as an impurity in the sample.⁸

As mentioned earlier, the system is metallic; and thus to avoid the skin depth problem of the rf power, the experiment is performed on a polycrystalline sample with small grain size. Because of the powdered sample, the line shape of the quadrupolar nucleus ^{59}Co is distributed over a wide range of frequency and this causes a decrease in the S/N ratio. To increase the S/N ratio a Tracor Northern NS570A signal analyzer is incorporated. The Knight shifts are measured with respect to the reference position (ν_R) of ^{59}Co resonance in the $\text{K}_3\text{Co}(\text{CN})_6$ solution.

A. Temperature variation of NMR spectra

Some typical ^{59}Co NMR spectra at different temperatures are shown in Fig. 1. At 300 K, the spectrum appears to be a second order quadrupolar splitted line of the central transition corresponding to a single cobalt site. Moreover, this spectrum experiences a huge amount of positive (low field) magnetic shift and therefore the position of the reference (ν_R) could not be indicated in the figure. Almost similar spectral features are observed down to 250 K. At 220 K,

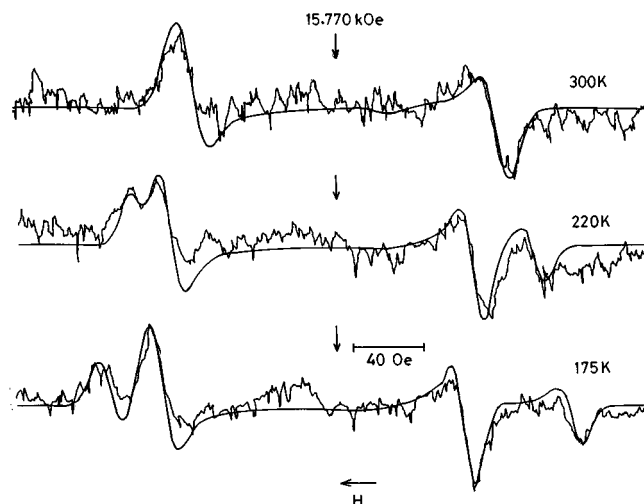


FIG. 1. Some typical first derivative spectra of ^{59}Co NMR absorption lines in NaCo_2O_4 at different temperatures, recorded at 16.2 MHz in a field swept mode. The vertical arrows (\downarrow) indicate the field position 15.77 kOe. Since the position of the reference ν_R (i.e., 16.2 MHz) is far away from the field range it could not be shown in the figure. The continuous line represents the fitted pattern obtained from the least square fitting of the experimental spectra as explained in the text.

structure appears on both side of the main pair of line shape. These structures have been found to be more and more resolved with the further lowering of temperature and, in fact, the separation between these two structures (i.e., the outer pair) increases as the temperature decreases. However, the separation between the inner pair remains the same through all temperatures. Spectrum at 175 K (Fig. 1) exhibits these features. As the behavior of the spectra is quite complex a detailed analysis of the line shape is needed to extract the hyperfine interaction parameters at each temperature.

B. Analysis of NMR line shape

In a system containing magnetic ions, the most general Hamiltonian¹¹ for a nucleus having spin $I > 1/2$ in the presence of a magnetic field \vec{H}_0 is written as

$$\mathcal{H} = \mathcal{H}_0 + \mathcal{H}_{\text{chem}} + \mathcal{H}_M + \mathcal{H}_Q, \quad (2.1)$$

where \mathcal{H}_0 is the Zeeman term, $\mathcal{H}_{\text{chem}}$ represents the temperature-independent chemical shift interaction including the contribution from orbital paramagnetism χ_{VV} in metals, which is analogous¹² to the Van Vleck paramagnetic susceptibility, \mathcal{H}_M is due to magnetic hyperfine interaction, and \mathcal{H}_Q is the electric quadrupolar interaction. Assuming that the principal axes of the electric field gradient (EFG) tensor and the magnetic shift tensor are coincident, the resonance condition¹³ in the case of the central transition may be written as

$$\begin{aligned} \nu_{1/2 \leftrightarrow -1/2} = \nu_R [1 + K_{\text{iso}} + K_{\text{ax}}(3 \cos^2 \theta - 1) \\ + K_{\text{aniso}} \sin^2 \theta \cos^2 \phi] - \frac{R}{6 \nu_0} [A(\phi) \cos^4 \theta \\ + B(\phi) \cos^2 \theta + C(\phi)], \end{aligned} \quad (2.2)$$

where θ and ϕ are the polar angles of \vec{H}_0 with respect to the principal axes system of EFG or magnetic shift tensor. $\nu_R = \gamma H_0/2\pi$, the resonance position of the reference, $\nu_0 = \nu_R(1 + K_{\text{iso}})$, $R = \nu_Q^2[I(I+1) - 3/4]$, and $K_{\text{iso}} = 1/3(K_1 + K_2 + K_3)$, $K_{\text{ax}} = 1/6(2K_3 - K_1 - K_2)$, $K_{\text{aniso}} = 1/2(K_2 - K_1)$. K_1 , K_2 , and K_3 are the principal values of the shift tensor and the principal axes system is chosen in such away that $K_1 < K_2 < K_3$. The terms $A(\phi)$, $B(\phi)$, and $C(\phi)$ are related to the asymmetry parameter (η) of the EFG tensor. Any contribution from $\mathcal{H}_{\text{chem}}$ is included within K_1 , K_2 , and K_3 .

Methods of determining the hyperfine interaction parameters have been developed for polycrystalline samples by Jones *et al.*¹⁴ for systems with axial symmetry and by Baugher *et al.*¹³ to cover cases of complete asymmetry. The absorption pattern of ^{59}Co NMR spectrum is

$$I(\nu) = \int_{-\infty}^{\infty} P(\nu') \exp[-(\nu - \nu')^2/2\beta^2] d\nu', \quad (2.3)$$

where 2β is referred to as the “intrinsic linewidth” and $P(\nu')$ is the normalized line shape function. If we consider that EFG and the magnetic shift tensors are axially symmetric then $P(\nu') = 1/2|d\nu'/d\cos\theta|^{-1}$, $-1 \leq \cos\theta \leq 1$. Using Eq. (2.2) with the restriction $\eta=0$ and $K_{\text{aniso}}=0$, an explicit calculation of $P(\nu')$ shows that the function possesses two singularities and a step at ν_H , ν_L , and ν_S , respectively, at different values of $\cos\theta$.¹⁴ The step is not usually detectable. It may be noted that the two singularities ν_H and ν_L correspond to the low and high field side divergent points of the line shape which is recorded in the field sweep mode. The fractional shifts of these two singularities with respect to ν_R are given by

$$K_H = \frac{\nu_H - \nu_R}{\nu_R} = K_{\text{iso}} - K_{\text{ax}} + \frac{R}{16\nu_R^2(1 + K_{\text{iso}})}, \quad (2.4a)$$

$$K_L = \frac{\nu_L - \nu_R}{\nu_R} = -K_{\text{iso}} - \frac{2K_{\text{ax}}}{3} + \frac{R}{9\nu_R^2(1 + K_{\text{iso}})} + \frac{4K_{\text{ax}}^2}{R}\nu_R^2. \quad (2.4b)$$

In order to extract the hyperfine interaction parameters at 300 K, K_H and K_L have been plotted against ν_R^{-2} as shown in Fig. 2. The linear variation of K_L vs ν_R^{-2} implies that K_{ax} is very small and thus the fourth term in the expression of K_L can be ignored. The infinite frequency extrapolated intercepts (Fig. 2) of these two plots provide two equations whose solutions give the value of K_{iso} and K_{ax} as 1.62 and 0.018 %, respectively. Using this value of K_{iso} , the quadrupolar interaction strength ν_Q has been calculated from the slope of K_H , K_L vs ν_R^{-2} lines. The average of these two is 1.02 ± 0.06 MHz.

The spectral feature varies widely at low temperatures and because of the difficulties of taking a sufficient number of data at different frequencies at a particular temperature, we have to depend only on the least square method of fitting the spectra using explicit equations (2.2) and (2.3). These theoretical spectra are shown by the continuous lines in Fig. 1. The nice agreement of the hyperfine interaction parameters obtained by fitting the experimental spectrum at 300 K with

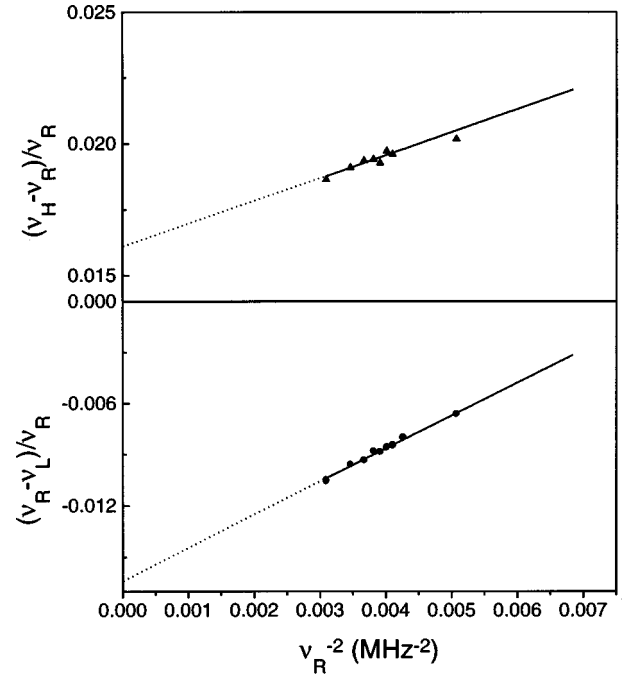


FIG. 2. The variation of K_H and K_L with respect to ν_R^{-2} at 300 K are shown in (a) and (b), respectively. K_H and K_L represent the fractional shifts of the two singularities of the line shape function with respect to ν_R as described in Eqs. (2.4a) and (2.4b). The dotted lines indicate the intercepts.

that found from graphical technique confirms the uniqueness of this least square fitting method of extracting the hyperfine interaction (HFI) parameters.

The experimental line shapes below 250 K could be best fitted with the theoretically generated line shape provided two inequivalent cobalt nuclei with different HFI's are considered. For convenience, we will call the ^{59}Co sites site 1 which contribute to the inner pair and site 2 corresponds to the outer pair of the line shape. It is known that the area under the spectrum is proportional to the number of nuclei. From the area under the theoretically generated spectra the ratio of the number of nuclei of site 1 to that of site 2 is calculated to be 2:1. The reality of the existence of these two cobalt sites has also been applied to extract the HFI parameters for all the spectrum above 250 K by the least square fitting method, though in the case of graphical analysis this 300 K spectrum is treated as an absorption line corresponding to a single cobalt site. Since the HFI parameters shows that at 300 K these two sites are equivalent so the consideration of the single site as is assumed in the graphical analysis does not make any difference. The equivalence of these two sites at 300 K agrees well with the room-temperature crystallographic structure.⁹ It is worthwhile to mention that ^{23}Na NMR also corresponds to a single species of sodium ion with well defined quadrupolar interaction parameters (Fig. 3) at 300 K.

III. TEMPERATURE DEPENDENCE OF ELECTRIC FIELD GRADIENTS

The temperature variation of the quadrupolar interaction parameter ν_Q which is proportional to the product of the quadrupolar moment of the nucleus under study and the EFG

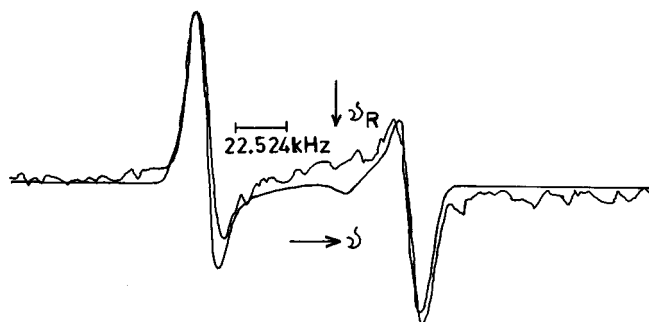


FIG. 3. ^{23}Na NMR spectrum in NaCo_2O_4 at 300 K recorded at 17 MHz. The continuous line represents the fitted pattern with $\nu_Q = 1.82$ MHz and $K_{\text{iso}} = 0.01\%$.

experienced by it is shown in Fig. 4. It implies that the EFG at site 1 is almost independent of temperature and that at site 2 decreases continuously with the increase of temperature in the temperature range 350–100 K.

Since EFG depends sensitively on the charge distribution around the nucleus in question, it reflects the structural aspects of the compound and provides information about ionicity and bonding.¹¹ Therefore, any change in EFG value should be related to either the structural phase change or the change in electronic state associated with the bonding. In the present case, for site 1 the charge distribution around cobalt nucleus remains unaltered which is the most general case. But for site 2, EFG changes 47% as temperature changes from 350 to 100 K. It can also be mentioned that temperature variation of EFG is found in some superconductors such as $\text{YBa}_2\text{Cu}_4\text{O}_8$, $\text{YBa}_2\text{Cu}_3\text{O}_7$ (Ref. 15) and in systems such as LaCoO_3 and NdCoO_3 which undergo electronic phase transition.¹⁶ In $\text{YBa}_2\text{Cu}_3\text{O}_7$, the change of EFG experienced by Cu2 site is found to be 0.5% as temperature changes from 270 to 20 K.

Nevertheless, the form of $\rho-T$,^{8,10} $\chi-T$ (Fig. 5), and EFG- T (Fig. 4) curves exclude the possibility of any structural phase transition of NaCo_2O_4 at low temperature. The recent result of heat capacity measurement in the single crystal also

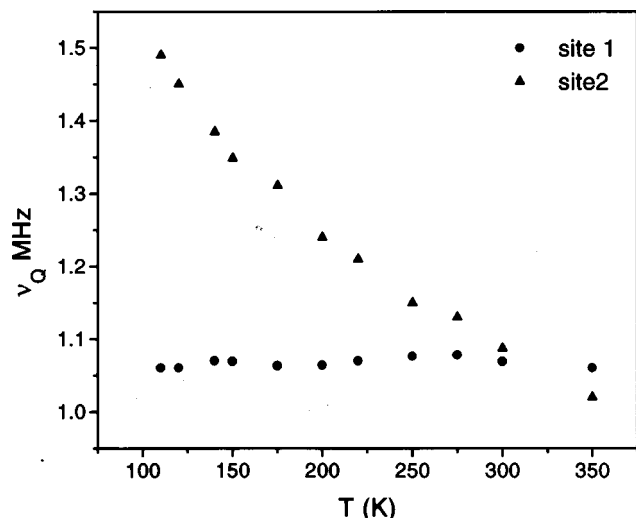


FIG. 4. The temperature variation of ν_Q experienced by the cobalt nucleus in NaCo_2O_4 for two species referred as site 1 and site 2 in the text.

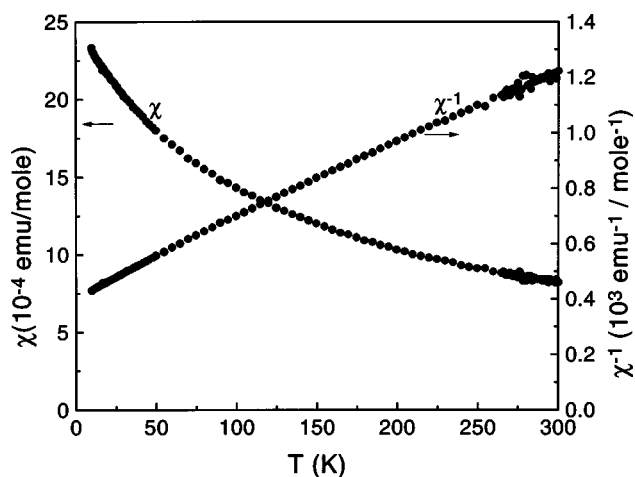


FIG. 5. The temperature variation of susceptibility (χ) and the inverse susceptibility (χ^{-1}) in the temperature range 10–300 K.

reveals no anomaly in the temperature range 10–300 K.¹⁷ In order to understand the huge amount of change in the EFG found for site 2 in NaCo_2O_4 , model calculations using e.g., a full potential linearized augmented plane wave (LAPW) band structure¹⁸ are needed.

IV. CONTRIBUTIONS TO THE SUSCEPTIBILITY AND ^{59}Co NMR SHIFT

A. Magnetic susceptibility

For a metallic system such as NaCo_2O_4 , the total susceptibility $\chi(T)$ as shown in Fig. 5 is given by

$$\chi(T) = \chi_s + \chi_{\text{dia}} + \chi_{VV} + \chi_d(T). \quad (4.1)$$

χ_s represents the Pauli paramagnetic component from s electrons. As some of the s electrons can be thought to be localized on the oxygen atoms and hence would not contribute to the electrical and magnetic properties.¹¹ However, there is no knowledge about the nature of s electrons from sodium ion. In comparison to the total susceptibility $\chi(T)$ at 300 K ($\approx 800 \times 10^{-6}$ emu/mole), the diamagnetic term χ_{dia} , to which the ion cores contribute, is a small correction. The term χ_{VV} has the origin in the temperature-independent orbital paramagnetism in metals which is analogous to the Van Vleck paramagnetic susceptibility in insulators. In a compound containing cobalt ion this generally has a large contribution.¹⁹ These three terms can be grouped together as χ_0 . The temperature-dependent spin paramagnetism $\chi_d(T)$ arises from the localized character of the d electrons. Therefore, Eq. (4.1) can be expressed as

$$\chi(T) = \chi_0 + C/(T - \Theta). \quad (4.2)$$

Applying Eq. (4.2) to the $\chi-T$ curve, with the least square fitting method, $\chi_0 = 1.61 \times 10^{-4}$ emu/mole, Curie constant $C = 0.276$ emu K/mole, and paramagnetic Curie temperature $\Theta = -118.5$ K are obtained. It is to be noted that C and Θ values for sodium compound are comparatively higher than those of potassium compound,⁸ whereas χ_0 is relatively smaller in case of former.

Assuming that all the cobalt sites contribute to the Curie constant equally, the effective magnetic moment ($p_{\text{eff}}\mu_B$) is

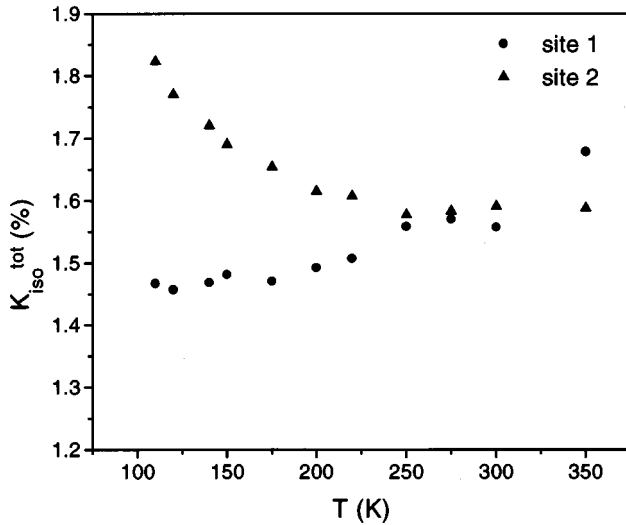


FIG. 6. The temperature variation of the total isotropic shift ($K_{\text{iso}}^{\text{tot}}$) of ^{59}Co NMR in NaCo_2O_4 for sites 1 and 2.

calculated to be about $1.05\mu_B/\text{Co}$. On the other hand, if we assume that only Co^{4+} spins contribute to the Curie constant as in KCo_2O_4 ,⁸ the effective magnetic moment is found to be around $1.49\mu_B$. This value is little bit smaller than $1.73\mu_B$ which is the spin only value of Co^{4+} in the low spin state with spin $S=1/2$. This may indicate that the electrons are partially localized, which is probable because in the oxide conductor, the carrier density is lower than in pure metal. The first possibility corresponds to the case where the cobalt ions behaves effectively as the $\text{Co}^{+3.5}$ ion. In this model the d band corresponding to the cobalt ion remains partially filled and it is expected to show conductivity. But in the second case the cobalt ions exist as Co^{3+} and Co^{4+} and in the octahedral crystal field the low spin (LS) state of these two ions are $S=0$ and $S=1/2$, respectively.²⁰ In this model also electrical conduction is expected arising from the partially filled t_{2g} band and due to this partial delocalization character of the d electrons the value of p_{eff} is less than that of the completely localized spin only value of $S=1/2$ ion. Thus both of these two models are equally probable to explain the conductivity and the susceptibility results. The d -band conductivity is also quite evident from the temperature variation of the resistivity data.¹⁰ Its strong anisotropic behavior in magnitude and in the T dependence as well indicates that CoO_2 layer is responsible for the conduction mechanism.

B. ^{59}Co NMR Knight shift

The effective magnetic field \vec{H} at the Co nucleus in NaCo_2O_4 may be written as

$$\vec{H} = \vec{H}_0 + \vec{H}_D + \vec{H}_{\text{hf}}^s + \vec{H}_{\text{hf}}^d + \vec{H}_{\text{chem}}, \quad (4.3)$$

where \vec{H}_0 is the applied magnetic field, \vec{H}_D is the dipolar field due to the electronic magnetic moment of all cobalt ions. \vec{H}_{hf}^s is the hyperfine field due to the contact interaction of the conduction s electrons and \vec{H}_{hf}^d may arise either from core polarization interaction by the d electrons as in transi-

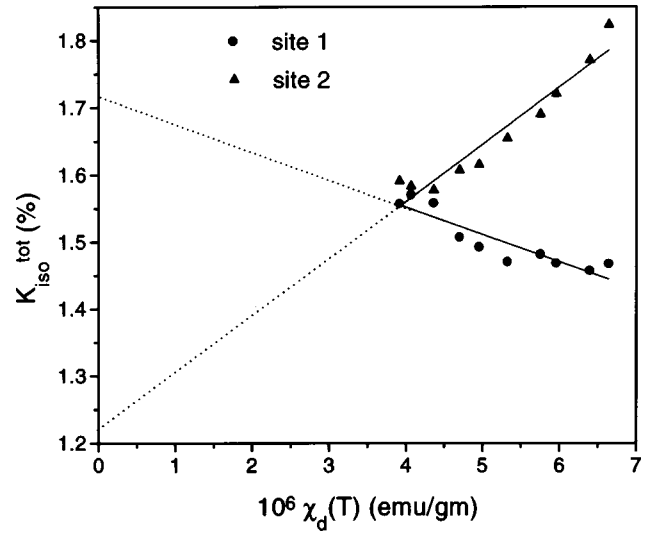


FIG. 7. The variation of $K_{\text{iso}}^{\text{tot}}$ against susceptibility $\chi(T)$ with temperature as an implicit parameter in the temperature range 300–100 K.

tion metals or due to transferred hyperfine interaction through intervening oxygen ion. \vec{H}_{chem} is the Van Vleck term which results from an induced orbital magnetic moment. Since the dipolar field \vec{H}_D does not contribute to the isotropic shift it may be discarded. Thus the isotropic Knight shift of ^{59}Co is given by

$$K_{\text{iso}}^{\text{tot}} = K_{vv} + K_s + K_d(T), \quad (4.4)$$

where K_{vv} is the dominating temperature-independent Van Vleck contribution, K_s is the temperature-independent contact hyperfine contribution of the conduction s electrons and K_d is the temperature-dependent shift due to the d spins of the magnetic ions. Each of these is considered to be proportional to the respective contribution of the susceptibility $\chi(T)$ of Eq. (4.1):²¹ $K_s = \alpha_s \chi_s$, $K_{vv} = \alpha_{vv} \chi_{vv}$, $K_d = \alpha_d \chi_d$. Since χ_s and χ_{vv} are independent of temperature and χ_d depends on temperature as discussed in the previous section, the total shift [Eq. (4.4)] can be written as

$$K_{\text{iso}}^{\text{tot}} = K_0 + K(T) = K_0 + \alpha_d \chi_d(T) \quad (4.5)$$

with $\alpha_d = (N\mu_B \gamma \hbar g)^{-1} A_{\text{hf}}^d$, where N is Avogadro's number, μ_B is the Bohr magneton, and A_{hf}^d is the total hyperfine coupling constant.

The temperature variation of the isotropic shift $K_{\text{iso}}^{\text{tot}}$ in the temperature range 350–100 K for both sites are shown in Fig. 6. The shift for site 1 increases with temperature, whereas that for site 2 decreases with the increase of temperature. In order to extract the temperature-independent contribution K_0 and the hyperfine coupling constant A_{hf}^d , the value of $K_{\text{iso}}^{\text{tot}}$ has been plotted against $\chi(T)$ as shown in Fig. 7, taking temperature as an implicit parameter. The values of K_0 for both sites can be obtained from Fig. 7 when $\chi(T)$ becomes zero and are listed in Table I. The hyperfine coupling constant A_{hf}^d as calculated from the slope $dK/d\chi$ of $K - \chi$ curve by using Eq. (4.5) are also given in Table I.

TABLE I. Temperature-independent shift, hyperfine coupling constant, and the observed and calculated ⁵⁹Co NMR linewidth ($\delta\nu$) in the NaCo₂O₄ system.

Cobalt site	K_0 (%)	A_{hf}^d (10^{-4} cm^{-1})	$\delta\nu_{\text{obs}}$ (kHz)	$\delta\nu_{\text{cal}}$ (kHz)
1	1.71	-7.489	11.2	6.21
2	1.22	15.624	11.6	7.06

1. Temperature dependent Knight shift

It is interesting to note that the coupling constant A_{hf}^d is positive for site 2 and negative for site 1. The negative coupling constant may be because of the inner s core polarization by the d band electrons as observed in transition metal, intermetallic compounds,²² and metallic oxide²³ containing transition elements. On the other hand, a coupling constant with positive sign observed for site 2 cannot be accounted for easily in a system having metallic character. It may be either due to the transferred hyperfine interaction between the spin of nucleus under question and the electron spin of the magnetic ion via intervening anion as was found in an insulating oxide such as Co₃O₄ (Ref. 19) or due to the strong s - d exchange mixing effects and/or a temperature-dependent orbital susceptibility as was found in hexagonal metals such as scandium, yttrium, and lanthanum.

If the first possibility is correct, then site 2 must belong to an insulator phase. This then leads to a conclusion that NaCo₂O₄ in the present study is composed of two phases; one belongs to the metallic phase and the other, an impurity phase, is an insulator. This is in contradiction with the x-ray diffraction results⁷ and the fact that both ⁵⁹Co and ²³Na NMR spectra at 300 K could be well explained on the basis of single species. On the other hand, the assumption of two inequivalent sites in a single metallic phase compound is more realistic, wherein two different electronic states around the cobalt nucleus exist. It is worthwhile to emphasize, that the out of plane resistivity (ρ_c) shows a crossover near 200 K from semiconducting to metallic phase with decreasing temperature, whereas the in-plane resistivity ρ_a shows a pure metallic behavior through all temperatures.¹⁰ Thus the NMR results along with the resistivity data demand further study of the electronic state of this interesting quasi-2D layered conductor.

Table II shows a list of the magnitude of the coupling constant A_{hf}^d of the cobalt nucleus in the different cobalt oxide systems which are insulating in character. In Co₃O₄, the Co³⁺ ion is in a diamagnetic state, in LaCoO₃ Co³⁺ ions

TABLE II. Comparison of the coupling constant A_{hf}^d in different cobalt oxide systems.

	NaCo ₂ O ₄		Co ₃ O ₄ ^a	LaCoO ₃ ^b	CoO ^c
	site 1	site 2			
A_{hf}^d 10^{-4} cm^{-1}	-7.48	15.62	13.0	37.5	107.6

^aFrom Ref. 19.

^bFrom Ref. 25.

^cR. G. Shulman [Phys. Rev. Lett. 2, 459 (1959)].

are in spin equilibrium between low spin ($S=0$) and high spin ($S=2$) states, whereas in CoO, Co²⁺ is a magnetic ion. Comparison of the coupling constant between these systems shows that if the nucleus under question resides within an ion which itself has an unpaired spin the magnitude of the hyperfine coupling constant is very high. This argument leads to the conclusion that the cobalt nucleus which is being probed in the NaCo₂O₄ system must belong to a cobalt site which is in a diamagnetic state. Though the ionicity of cobalt in NaCo₂O₄ is not known unambiguously, the above result suggests that some of the cobalt ions are in a diamagnetic state and from susceptibility it is obvious that the rest are the magnetic ions. This result can be incorporated with the second model as described earlier to explain the conductivity and susceptibility data that it consists of equal number of Co³⁺ and Co⁴⁺ ions and in the octahedral ligand, Co³⁺ and Co⁴⁺ ions are in the LS state with spin $S=0$ and $S=1/2$, respectively.

2. Contributions to the linewidth

We shall now discuss the different contribution to the intrinsic linewidth of the ⁵⁹Co NMR spectrum. This intrinsic linewidth obtained from a least square fitting method does not show any temperature dependence. Apart from the field inhomogeneities arising from the variation of the demagnetizing field within a given particle and between different particles, the NMR linewidth is mainly governed by nuclear-nuclear dipolar interaction and time-dependent electron-nuclear magnetic interaction.²⁴ The calculated value of the linewidth (10.8 kHz) from the nuclear-nuclear dipolar contribution in ²³Na NMR is very close to the observed linewidth (10 kHz). This is consistent with the fact that the ²³Na NMR line does not experience any magnetic shift. In the case of ⁵⁹Co NMR the nuclear-nuclear dipole contribution to the linewidth ~ 5.08 kHz, the demagnetization correction at 16.2 MHz is ~ 0.87 kHz, whereas the experimental linewidth for sites 1 and 2 are 11.2 and 11.6 kHz. These results together with the temperature-dependent shift suggest a non-zero contribution to the linewidth due to the paramagnetic ion. An estimate for the NMR linewidth $\delta\nu$ for a nucleus interacting with a fluctuating magnetic field is given by Moriya²⁴ with the result

$$\delta\nu \approx 2(1/6\pi)^{1/2} (A_{\text{hf}}^d)^2 S(S+1) / 3\hbar^2 \omega_e,$$

where S is the electron spin, γ is the nuclear gyromagnetic ratio, and ω_e , the exchange frequency is defined by $\omega_e^2 = (2/3)(J/\hbar)^2 ZS(S+1)$, where Z is the number of nearest-neighbor magnetic ions to the magnetic Co⁴⁺ ion and J is the exchange constant. The value of J has been estimated as 54.51×10^{-16} erg using $\theta = -118.5$, $Z=6$, $S=1/2$ from the equation $J = 3k\theta/2S(S+1)Z$. Thus the exchange frequency becomes $\omega_e \approx 1.097 \times 10^{13} \text{ sec}^{-1}$. Using the coupling constant as in Table I, the full linewidth for sites 1 and 2 are estimated as 0.254 and 1.109 kHz, respectively, which are smaller than nuclear-nuclear dipole contribution. Table I shows that the total calculated full linewidth ($\delta\nu_{\text{cal}}$) is smaller than the observed linewidth ($\delta\nu_{\text{obs}}$). The discrepancy

between the two values may be due to an extra broadening caused by the skin depth problem of the rf power in this metallic system.

3. Temperature-independent shift

The temperature-independent shift K_0 for sites 1 and 2 are ~ 1.71 and 1.22% , respectively (Table I). It is worthwhile to mention that ^{59}Co NMR in perovskites such as LaCoO_3 , PrCoO_3 , etc., exhibits similar large temperature-independent shifts which accounted for Van Vleck temperature-independent susceptibility.^{16,25} In the present case, the temperature-independent shifts in principle are the sum of K_{vv} and K_s as described in Eq. (4.4). In a metallic oxide such as V_2O_3 , s electrons do not contribute to the electrical and magnetic properties since they are considered to be localized to the oxygen atoms.²³ A similar argument when applied to NaCo_2O_4 reveals that either $K_s = 0$ or it is negligible in comparison to K_0 . So, $K_0 \approx K_{vv}$. The Van Vleck contribution K_{vv} is given by²⁵ $K_{vv} = 2\langle r^{-3} \rangle \chi_{vv} / N$ where $\chi_{vv} = 16N\mu_B^2\kappa^2/\Delta$ and $\langle r^{-3} \rangle$ is the average value of r^{-3} over a single $3d$ orbital, N is the Avogadro number, Δ is the crystal field splitting, μ_B is the Bohr magneton, and κ is the orbital reduction factor which is defined by the matrix element of the z component of the angular momentum between t_{2g} and e_g orbitals.

Using the free ion value $\langle r^{-3} \rangle = 6.7$ atomic unit corresponding to Co^{3+} ion and K_{vv} as shown in Table I, χ_{vv} have been calculated to be 1.142×10^{-4} emu/gm-ion and 0.812×10^{-4} emu/gm-ion for sites 1 and 2, respectively. The term Δ/κ^2 then for sites 1 and 2 comes out to be 4.5 and 6.3 eV, respectively. These are consistent with the values of Δ/κ^2 in LaCoO_3 (3.8 eV) (Ref. 25) and Co_3O_4 (4.2 eV) (Ref. 26) systems where also Co^{3+} ions are in oxygen octahedra.

V. CONCLUSION

The temperature variation of the susceptibility and conductivity results can be explained equally with the help of two models. The first possibility is that all the cobalt ions contribute equally to the susceptibility and thus they behave effectively as $\text{Co}^{+3.5}$ ions. The second possibility is that the

cobalt ions exist as Co^{3+} and Co^{4+} and in the octahedral ligands the LS state of these two ions are $S=0$ and $S=1/2$, respectively. ^{59}Co NMR results suggest that in NaCo_2O_4 there are two inequivalent Co sites in the ratio 2:1. The temperature variation of the EFG experienced by site 1 remains almost independent of temperature, whereas that of site 2 increases with the decrease of temperature. The isotropic shift has two parts. The large temperature-independent shift has been accounted for by field induced orbital susceptibility. The temperature-dependent isotropic Knight shift of these two sites behaves differently. The negative sign of $dK/d\chi$ for site 1 may be because of the inner core s electron polarization by the d band electrons indicating the d band conduction in this system. On the other hand, the positive sign of $dK/d\chi$ for site 2 could not be accounted for directly for a metallic system such as NaCo_2O_4 . A positive hyperfine coupling constant is generally observed to be either due to transferred hyperfine interaction as found in the case of an insulator such as Co_3O_4 or due to strong s - d exchange interaction and/or temperature-dependent orbital susceptibility. The former possibility leads to an indication of the existence of an insulating phase as an impurity in the otherwise metallic phase. But it is in contradiction with the x-ray results. A comparison of the magnitude of the hyperfine coupling constant with those of other cobalt oxides suggests that the nucleus which is being probed by NMR resides within a diamagnetic cobalt site. This result together with the susceptibility emphasizes the presence of the Co^{3+} ion with $S=0$ and the magnetic Co^{4+} ions. Finally the different contributions to the linewidth have been calculated. It is mainly governed by nuclear-nuclear dipole interaction and contributions from a fluctuating magnetic field and demagnetization correction are of the same order of magnitude. A better understanding of the conduction mechanism would emerge from the study of the dynamic behavior which is being reflected in the relaxation phenomenon.

ACKNOWLEDGMENTS

We are very much thankful to the Director, Saha Institute of Nuclear Physics, Calcutta for providing us the necessary infrastructural facility.

- ¹M. Hase, I. Terasaki, and K. Uchinakura, Phys. Rev. Lett. **70**, 3651 (1993); M. Azuna, Z. Hiroi, and M. Takano, *ibid.* **73**, 3463 (1994).
- ²D. C. Johnston, J. Low. Temp. Phys. **25**, 145 (1976).
- ³M. Steinbruck and A. Feltz, J. Mater. Sci. Lett. **11**, 216 (1992).
- ⁴S. Kondo, D. C. Johnston, C. A. Swenson, F. Borsa, A. V. Mahajan, L. L. Miller, T. Gu, A. I. Goldman, M. B. Maple, D. A. Gajewski, E. J. Freeman, N. R. Dilley, R. P. Dickey, J. Merrin, K. Kojima, G. M. Luke, Y. J. Uemura, O. Chmaissem, and J. D. Jorgensen, Phys. Rev. Lett. **78**, 3729 (1997).
- ⁵G. R. Stewart, Rev. Mod. Phys. **56**, 755 (1984).
- ⁶Y. Maeno, H. Hashimoto, K. Yoshida, S. Nishizaki, T. Fujita, J. G. Bednorz, and F. Lichtenberg, Nature (London) **372**, 532 (1994).

- ⁷T. Tanaka, S. Nakamura, and S. Iida, Jpn. J. Appl. Phys., Part 2 **33**, L581 (1994).
- ⁸S. Nakamura, J. Ohtake, N. Yonezawa, and S. Iida, J. Phys. Soc. Jpn. **65**, 358 (1996).
- ⁹M. Von Jansen and R. Hoppe, Z. Anorg. Allg. Chem. **408**, 104 (1974).
- ¹⁰I. Terasaki, Y. Sasago, and K. Uchinokura, Phys. Rev. B **56**, R12 685 (1997).
- ¹¹*NMR 31, Solid-State NMR II Inorganic Matter*, edited by P. Diechi, E. Fluck, H. Gunther, R. Kosfeld, and J. Seeling (Springer-Verlag, Berlin, 1994).
- ¹²R. Kubo and Y. Obata, J. Phys. Soc. Jpn. **11**, 547 (1956).
- ¹³J. F. Baugher, P. C. Taylor, T. Oja, and P. J. Bray, J. Chem. Phys. **50**, 4914 (1969).

- ¹⁴W. H. Jones, Jr., T. P. Graham, and R. G. Barnes, Phys. Rev. **132**, 1898 (1963).
- ¹⁵H. Zimmermann, M. Mali, D. Brinkmann, J. Karpinski, E. Kaldis, and S. Rusiecki, Physica C **159**, 681 (1989).
- ¹⁶M. Bose, A. Ghoshray, A. Basu, and C. N. R. Rao, Phys. Rev. B **26**, 4871 (1982), and references therein.
- ¹⁷N. Miyamoto, K. Segawa, Y. Ando, T. Kawata, and I. Terasaki, Meeting Abstract Phys. Soc. Jpn. **53**, 668 (1998) (In Japanese).
- ¹⁸P. Blaha, K. Schwarz, and P. Herzig, Phys. Rev. Lett. **54**, 1192 (1985).
- ¹⁹K. Miyantani, K. Kohn, H. Kamimura, and S. Iida, J. Phys. Soc. Jpn. **21**, 464 (1966).
- ²⁰John B. Goodenough, *Magnetism and the Chemical Bond* (Wiley, New York, 1963).
- ²¹P. J. Segransan, Y. Chabre, and W. G. Clarks, J. Phys. F **8**, 1513 (1978).
- ²²A. M. Clogston and V. Jaccarino, Phys. Rev. **121**, 1357 (1961).
- ²³E. D. Jones, Phys. Rev. **137**, A978 (1965).
- ²⁴T. Moriya, Prog. Theor. Phys. **16**, 641 (1956).
- ²⁵M. Itoh and I. Natori, J. Magn. Magn. Mater. **140-144**, 2145 (1995).
- ²⁶H. Kamimura, J. Phys. Soc. Jpn. **21**, 484 (1966).